

# Isolation and Control of Voids and Void-hillocks during Molecular Beam Epitaxial Growth of HgCdTe

D. CHANDRA,<sup>1,2</sup> F. AQARIDEN,<sup>1</sup> J. FRAZIER,<sup>3</sup> S. GUTZLER,<sup>1</sup>  
T. ORENT,<sup>1</sup> and H.D. SHIH<sup>1</sup>

1.—DRS Infrared Technologies, L.P., 13532 North Central Expressway, Dallas, TX 75243.  
2.—e-mail dchandra@drs-irtech.com. 3.—Raytheon TI Systems, P.O. Box 655936,  
Dallas, Texas 75265

Formation of small voids and defect complexes involving small voids during the molecular beam epitaxial growth of mercury cadmium telluride on cadmium zinc telluride was investigated. Some of these defects were demonstrated to form away from the substrate-epi interface. Other defects were demonstrated to close before reaching the top surface without leaving any perturbations on the surface, thus remaining completely hidden. The voids, which formed away from the substrate-epifilm fixed interface, nucleated on defects introduced into the film already grown, leading to the formation of defect complexes, unlike the voids which nucleated at the substrate-epifilm fixed interface. These defect complexes are decorated with high density dislocation nests. The voids which closed before reaching the film surface usually also nucleated slightly away from the film-substrate interface, continued to replicate for a while as the growth progressed, but then relatively rapidly closed off at a significant depth from the film surface. These voids also appeared to form defect complexes with other kinds of defects. Correlations between these materials defects and performance of individual vertically integrated photodiode (VIP) devices were demonstrated, where the relative location of these defects with respect to the junction boundary appears to be particularly important. Elimination or reduction of fluctuations in relative flux magnitudes or substrate temperature, more likely during multi-composition layer growth, yielded films with significantly lower defect concentrations.

**Key words:** MBE, HgCdTe, hillocks, IR detectors

## INTRODUCTION

Void defects were demonstrated to form away from the substrate-epifilm interface during the molecular beam epitaxial growth of mercury cadmium telluride on cadmium zinc telluride substrates.<sup>1</sup> These were smaller in size compared to voids, which nucleated at the substrate-epifilm interface, which were also observed. Once nucleated, voids usually replicated all the way to the surface even if the flux ratios were modified to prevent additional nucleation of voids.

During the present investigations, additional details of these smaller voids were studied. It was observed that these voids usually existed as defect complexes, where the additional defect in each complex consisted of a hillock. Furthermore, several dif-

ferent varieties of these voids were observed, with some nucleating very close to the top surface and some nucleating deep within the film. Among the latter, in some cases, voids were observed to close before reaching the film surface.

## EXPERIMENTAL PROCEDURES

The HgCdTe films were grown on (211)B oriented CdZnTe substrates in a custom MBE system manufactured by DCA Instruments. Some HgCdTe films were also grown in the Riber 2300 MBE system. The films were grown on near lattice matched CdZnTe to reduce or eliminate the misfit dislocation density in the epilayers. The substrates were mostly supplied by DRS Infrared Technologies. A few substrates delivered by Japan Energy (NIMTEC) were also employed. The substrates were etched in a 1% bromine-methanol solution to remove approximately 5  $\mu\text{m}$  of the surface, followed by rinsing in a methanol bath and

(Received February 1, 2000; accepted February 22, 2000)

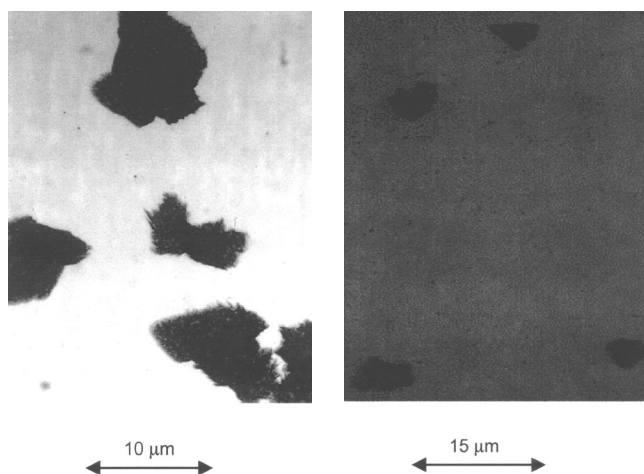


Fig. 1. Voids observed in films which were grown at 180°C. Growth rate between 2 and 3  $\mu\text{m/hr}$ . Separate sources of Te, CdTe, and Hg.

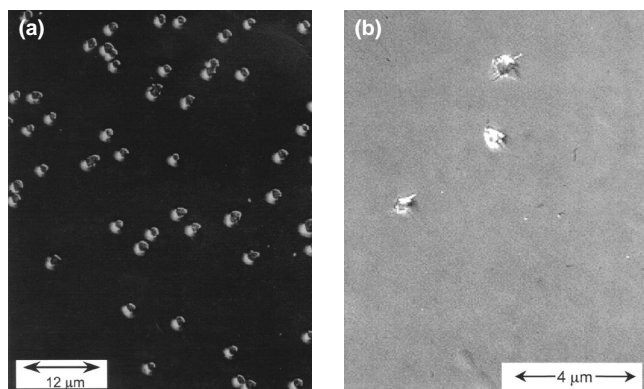


Fig. 2. (a) Defects which appear to be voids inside hillocks. (b) Defect complexes where the hillocks appear to be associated with void edges.

drying in nitrogen. The drying was performed immediately after the rinse. Detailed discussion of the MBE growth and processing procedures employed can be obtained elsewhere.<sup>1-5</sup>

## RESULTS AND DISCUSSIONS

Figure 1 displays the types of voids observed in these films. The voids vary both in size and shape. The smaller voids appear to be less irregular or more circular in cross-section. But, each of the smaller voids appears also to be a part of a defect complex. Figure 2 displays typical defect complexes. These appear to be voids existing inside hillocks, or void-hillock complexes. These defect complexes appear to be associated with a nest of 'decorating' dislocations. This becomes apparent upon defect etching small sections of films such that the location of each individual defect complex is relatively precisely correlated during the etching process. This is displayed in Fig. 3. For the most part, these nests were complex, consisting of >10 individual etch pits, frequently ranging to >100 individual etch pits. Interestingly, however, each component of these defect complexes, when they existed unaccompanied with the other, never displayed an accompanying dislocation nest. This is displayed in Fig. 4, showing typical unaccompanied (relatively large) voids following defect etching, and in Fig. 5, showing typical unaccompanied hillocks following defect etching.

The large voids, with sizes usually greater than 5  $\mu\text{m}$ , nucleated at the substrate-epi interface. The smaller voids appeared, however, to nucleate away from the substrate-epi interface. Direct evidence of these voids on cleaved cross-sections of MBE films has been obtained earlier<sup>1</sup> and reproduced in Fig. 6. As displayed, usually the voids, once nucleated either at the substrate-epi interface or away from it, continued to replicate through to the top surface of the films.

The behavior described above has generally been observed earlier. However, during the present investigations, for a significant number of films a fraction of the voids appears to close before reaching the film surface. Figure 7 displays several examples. Here the

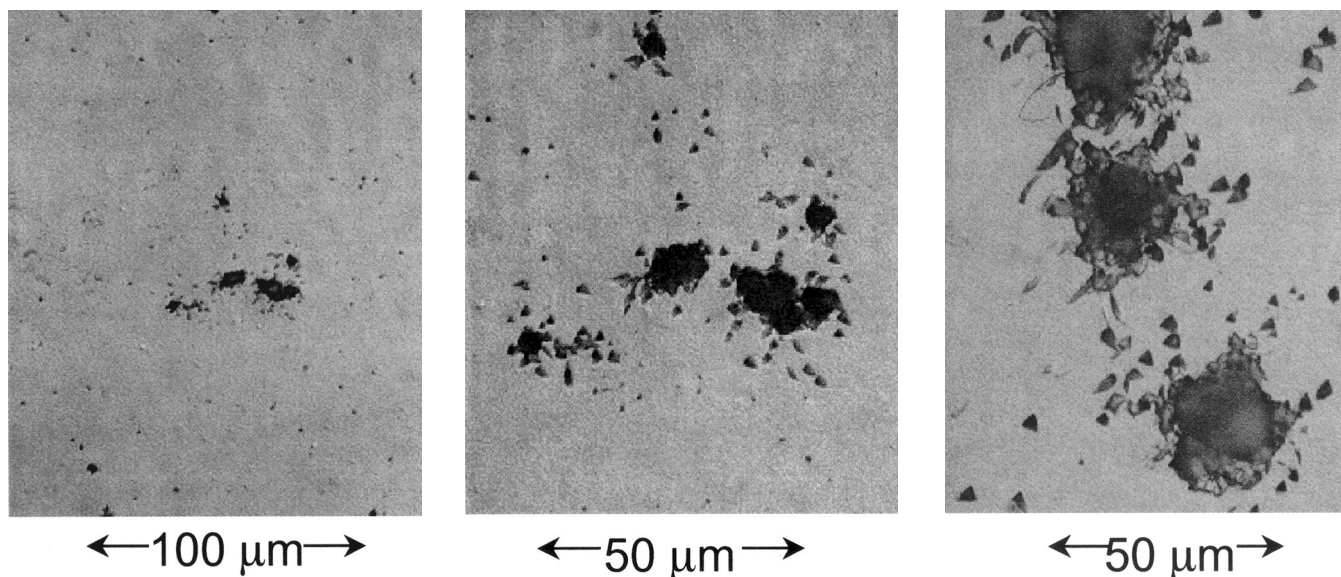


Fig. 3. Dislocation etching of films containing void-hillocks. Strong "nests" of dislocation etch pits appear to be visible around each void-hillock complex.

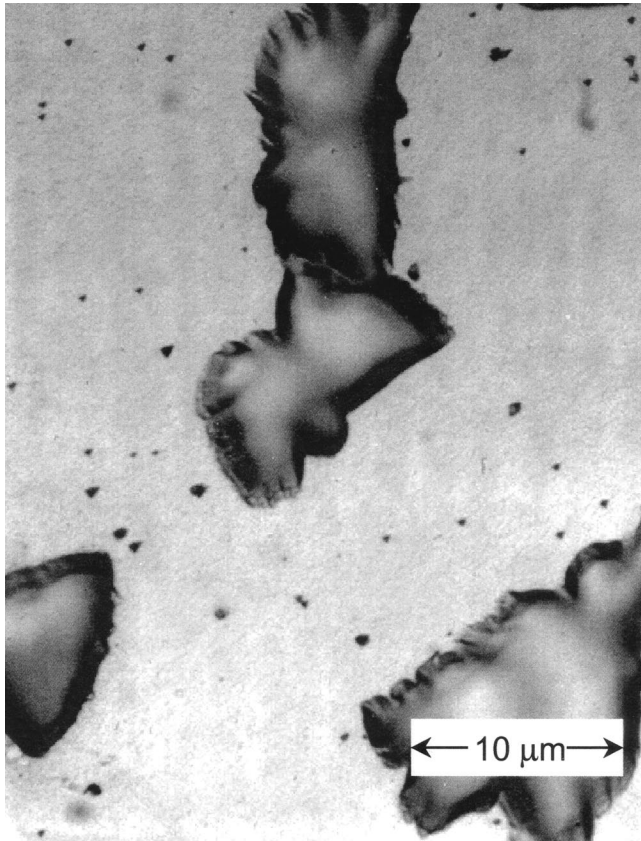


Fig. 4. Dislocation etching of films containing large but simple voids. The dislocation density appears low and independent of the location of the void defects.

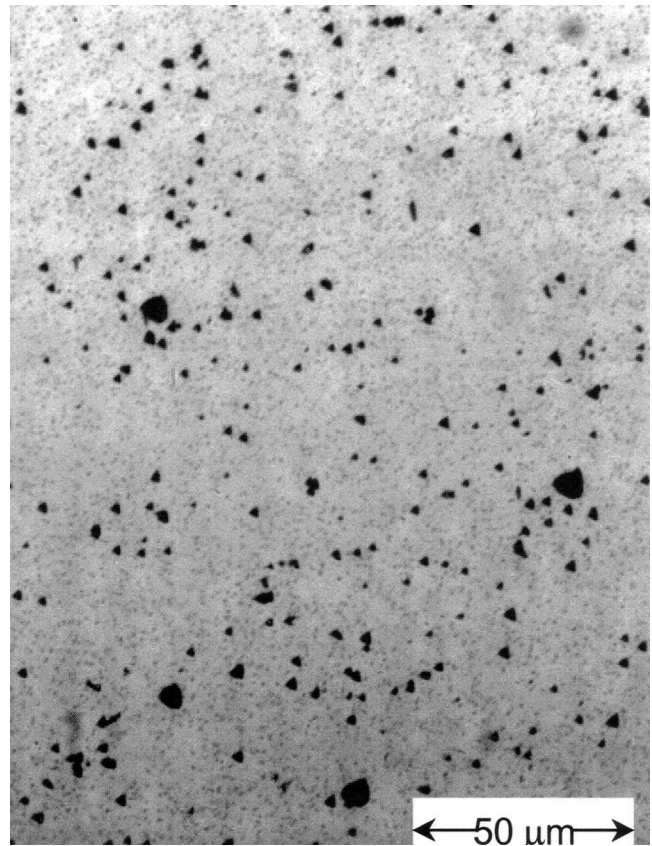


Fig. 5. Dislocation density of films containing hillocks. The dislocation density has increased, but does not appear to be associated with individual hillocks.

voids nucleated slightly away from the film-substrate interface, continued to replicate for a while as the growth progressed, but then relatively rapidly closed off at significant depths from the film surface. The whole sequence was completed before two-thirds of the film growth was completed.

Examination of the top surface of these films does not reveal any indication of voids within the depth of the films. These only become apparent upon examination of cleaved cross-section of these films. Voids, which close during growth, can nucleate either at the interface or away from the interface. Furthermore, these voids may not always be leaving any “finger-prints” on the top surface. Defect etching these films did not indicate a presence of nesting dislocations. However, void density increased upon selective and progressive removal of the epi film. When defect etching was performed following a partial removal of the film, dislocation nests were observed decorating these voids in some cases. An example is displayed in Fig. 8. No nests or decorative pattern of dislocations were observed upon defect etching the top surface of a selected small section of a MBE film (Fig. 8a). Upon removal of approximately half of the film thickness by chemical etching, this section was then defect etched. A number of dislocation nests springs into view (Fig. 8b and c).

No direct correlation between the location of these

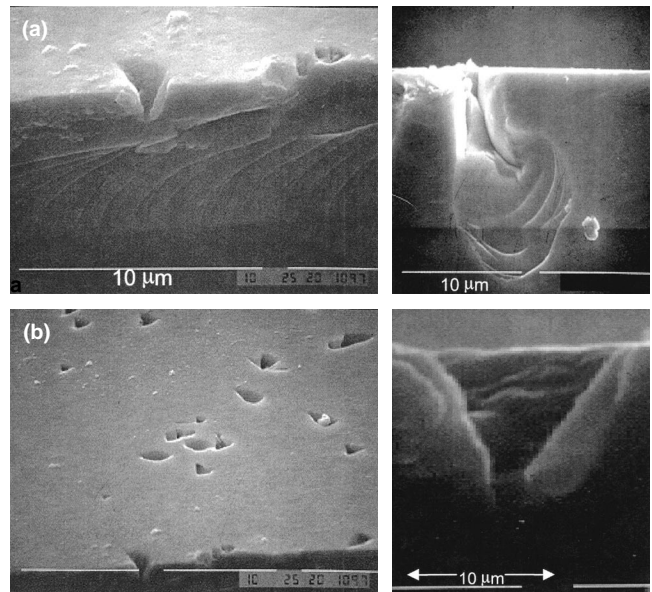


Fig. 6. Cross-sectional and three dimensional SEM microphotographs of void defects nucleated at various stages of MBE growth: at the growth interface, in the middle of the growth run, near the end of the growth run (a,b).

defects and device performance was possible during the earlier investigation. However, during the present investigations, a partial correlation between these

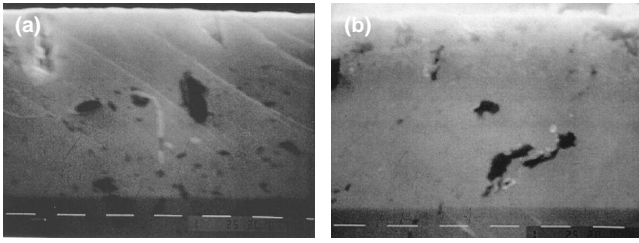


Fig. 7. Cross-sectional SEM microphotograph of void defects which "closed" before the end of the growth run. These voids will be completely hidden and not apparent from the top surface.

defect complexes and vertically integrated photo-diode device performance was attempted. Figure 9 displays 3 specific cases of diodes fabricated on a LWIR MBE film with a cutoff at 77 K of 10.0  $\mu\text{m}$ . The diode junction boundary is clearly marked in the photograph. When the void-hillock complex, clearly apparent in the micrograph, is located at the junction boundary (Fig. 9a), it leads to a failed diode, as evident by very low magnitudes of the performance parameters of impedance-area products, both without bias ( $R_0A$ ) and with bias ( $R_{50}A$ ). Both these parameters stayed at less than 5% of their expected magnitudes of 100  $\text{ohm}\cdot\text{cm}^2$  and  $>5 \times 10^4 \text{ ohm}\cdot\text{cm}^2$ , respectively. When the defect is located significantly away from the junction boundary, but still within the active area (Fig. 9b), the zero bias impedance-area product is less affected, decreasing only to 30  $\text{ohm}\cdot\text{cm}^2$ ; but the 'reverse bias' impedance-area product ( $R_{50}A$ ) is still severely affected, staying at 70  $\text{ohm}\cdot\text{cm}^2$ . The best performing diodes do not appear to be associated with visible defects. An example is shown in Fig. 9c. Here the zero bias impedance-area product was measured at 105  $\text{ohm}\cdot\text{cm}^2$ , whereas the reverse bias impedance-area product ( $R_{50}A$ ) was determined to be  $9.8 \times 10^4 \text{ ohm}\cdot\text{cm}^2$ .

These defects arise from fluctuations in growth

conditions, some of which were qualitatively discussed during an earlier report.<sup>1</sup> With increasing Hg flux, or with decreasing substrate temperature, the growth morphology transitions from voids associated with low dislocation density, to the optimal growth window displaying few voids, but still with low dislocation density, to formation of twins (hillocks) and increasing dislocation density.<sup>1,3,4</sup> Complex conditions emerge when fluctuations occur during growth, either in the relative magnitude of the Hg flux or in the substrate temperature, to force transition from one regime to another regime. If, for example, the growth transitions from Hg rich to Hg deficient, then twins or hillocks will form first, followed by void nucleation. The hillocks already formed may serve as nucleation sites for these void defects, inducing void formation on hillocks.

For conditions, where the growth transitions again back strongly to Hg rich, void closure may become a possibility. The precise conditions under which this can occur remain still to be established. Nevertheless, these conditions will be more likely during growth of multi-layer and multi-composition films, where it will be necessary to change relative flux magnitudes and substrate temperature to transition from the growth of a layer of one composition to a layer of another composition.

Ensuring maintenance of the growth within the same regime during the entire process can be demonstrated to drastically decrease the concentration of both the void-hillock complex defects and the "hidden" voids. Figure 10 displays the void density (Fig. 10a) and the dislocation density (Fig. 10b) of a MBE growth run maintained within the same growth regime. When approximately half of the film thickness was removed, and this film was then defect etched, no nests of dislocations or additional voids become apparent (Fig. 10c).

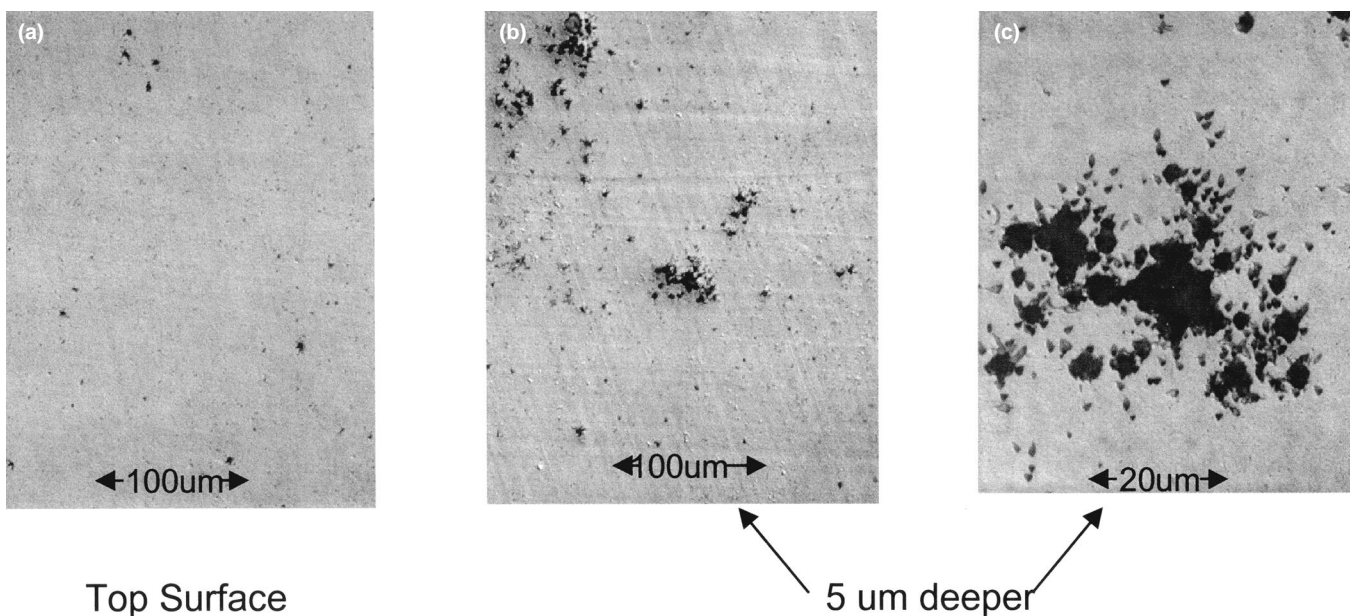


Fig. 8. Dislocation etching of a MBE film containing "hidden" voids. (a) Dislocation nests are not apparent on the top surface, but become apparent upon removal of half of the film (b,c).

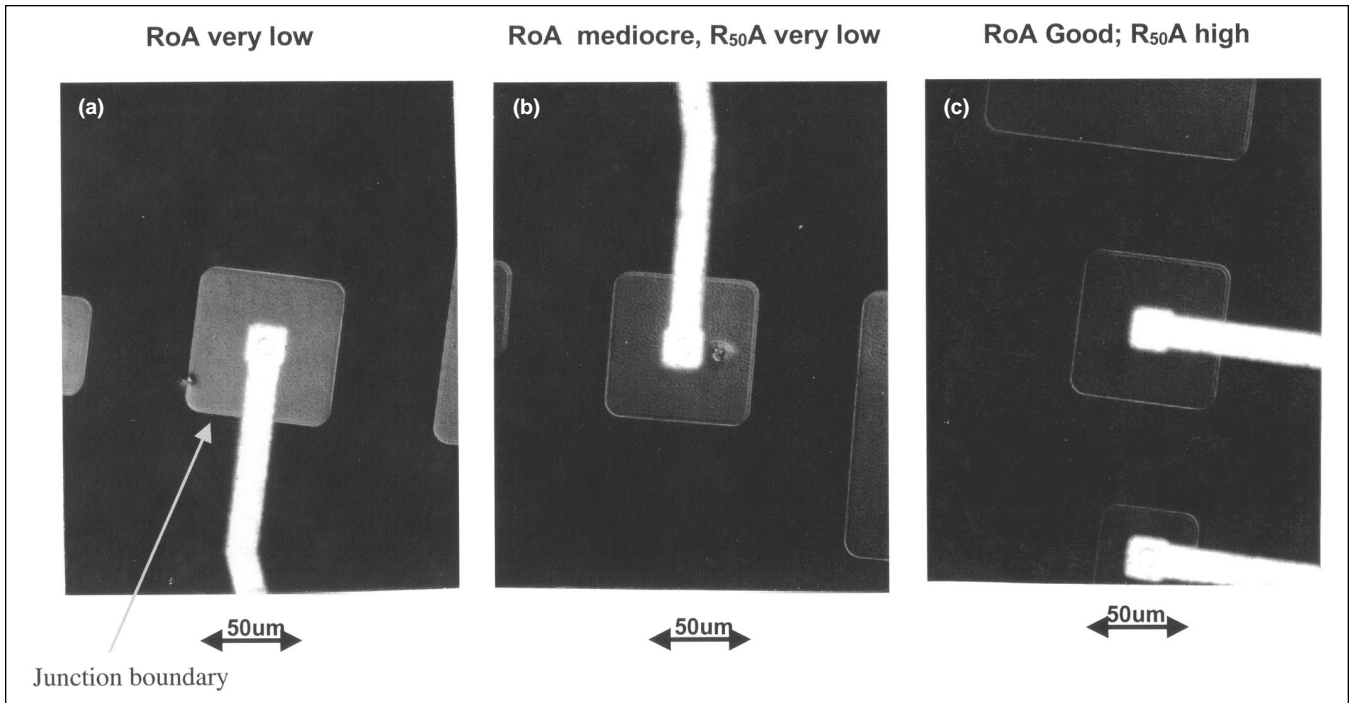


Fig. 9. Specific cases of diodes fabricated on a LWIR MBE film with a 77 K cutoff of 10.0  $\mu\text{m}$ . The diode junction boundary is clearly apparent. Examples of (a) failed diode, when the void-hillock complex is located at the junction boundary, (b) partially failed diode where the void-hillock complex is located away from the junction boundary, but still within the active area, (c) best diode, not associated with visible defect. Details of diode performances are given in the text.

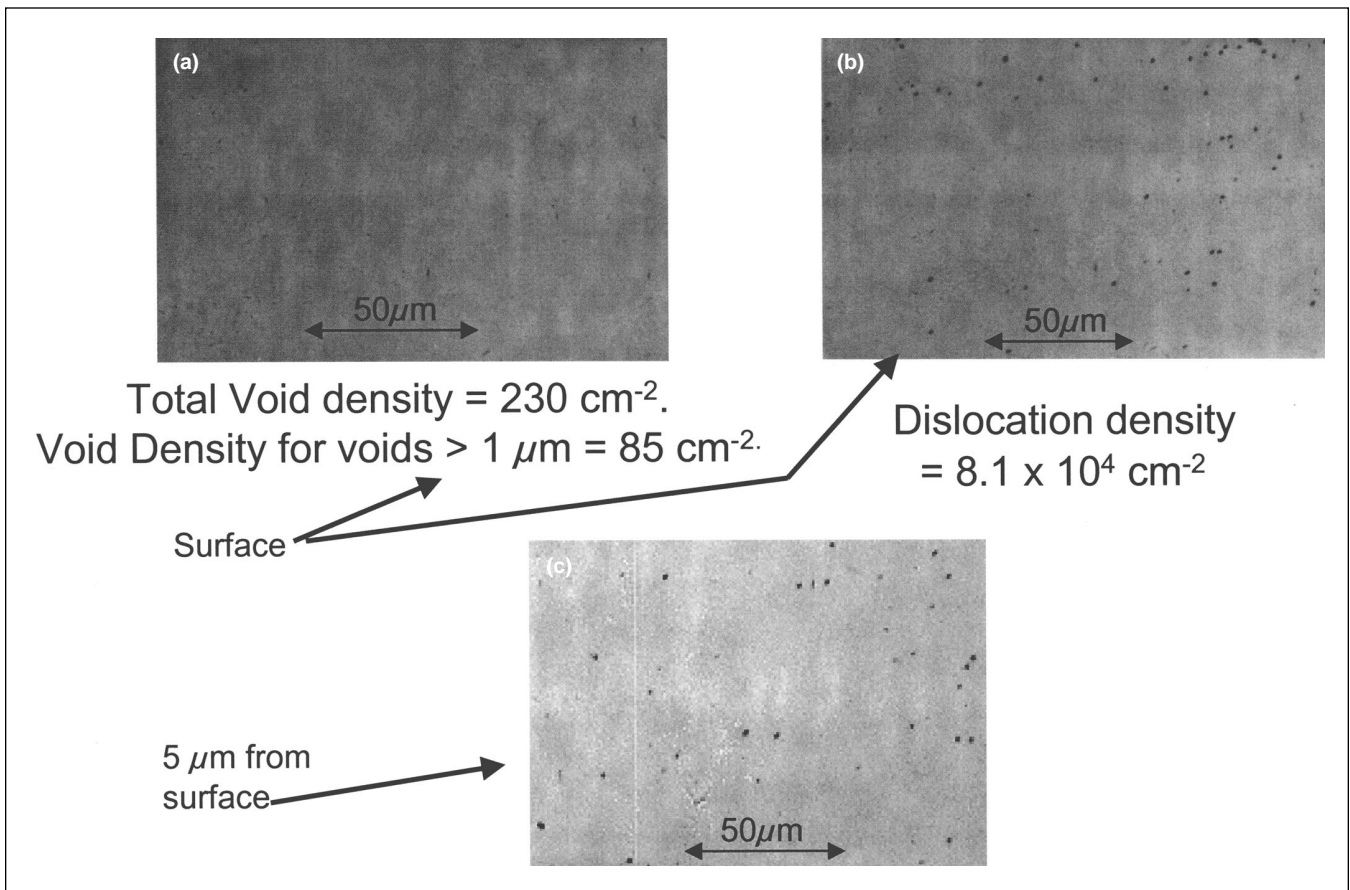


Fig. 10. (a) Void density and (b) the dislocation density of a MBE growth run maintained within the same growth regime; and (c) dislocation density when half of the film is removed.

## CONCLUSIONS

Void defects during MBE growth of HgCdTe can nucleate at the substrate-epifilm interface as well as away from it. The latter kind of void defects is smaller in size compared to voids nucleating at the interface and appears to be usually present as a defect complex, leading to the formation of an associated decorative dislocation nest. Both kinds of voids usually penetrate through to the surface of the film. However, examples where voids have closed before reaching the top surface of the film have been observed. No indications of these hidden voids can be observed by examining the top surface of the films. Elimination of fluctuations in growth conditions, usually likely to be associated with multi-layer and multi-composition films, eliminated the formation of these complex defects.

## ACKNOWLEDGEMENTS

The work was supported in part by the Advanced Sensors Consortium sponsored by the U.S. Army Research Laboratory under Cooperative Agreement DAAL01-96-20-0001.

## REFERENCES

1. D. Chandra, H.D. Shih, F. Aqariden, R. Dat, S. Gutzler, M.J. Bevan, and T. Orent, *J. Electron. Mater.* 27, 640 (1998).
2. J.P. Faurie, S. Sivananthan, and P.S. Wijewarnasuriya, *SPIE Conf. Proc.* 1735, 141 (1992).
3. M. Zandian, J.M. Arias, J. Bajaj, J.G. Pasko, L.O. Bubulac, and R.E. DeWames, *J. Electron. Mater.* 24, 1207 (1995).
4. J.M. Arias, J.G. Pasko, M. Zandian, S.H. Shin, L.O. Bubulac, R.E. DeWames, and W.E. Tennant, *J. Electron. Mater.* 22, 1049, (1993).
5. M.J. Bevan, W.M. Duncan, G.H. Westphal, and H.D. Shih, *J. Electron. Mater.* 25, 1371 (1996).